DOI: 10.22661/AAPPSBL.2019.29.5.52

# Molecular Switches Regulating Assembly Transitions of Biological Molecules: Tubulin, Amylin and Lipids

DAE-WOONG JEONG[1], SUHO LEE[1], JUNCHEOL LEE[1], HYUNWOO JANG[1], SUNGMUN LEE[2], MYUNG CHUL CHOI[1]
[1]DEPARTMENT OF BIO AND BRAIN ENGINEERING, KAIST, DAEJEON, KOREA;
[2]DEPARTMENT OF BIOMEDICAL ENGINEERING, KHALIFA UNIVERSITY OF SCIENCE AND TECHNOLOGY, ABU DHABI, UAE

This article presents recent works developing a fundamental understanding of structures and interactions of supramolecular assemblies of biological molecules, in particular, tubulin, amylin and lipids, of which the assembly transition is regulated by molecular switches – tau, taxol, cholesterol, SPAN 80 and lipoic/ascorbic acids. Nanometer to many micrometer scaled structures are solved by combining reciprocal space and real space data resulting from X-ray scattering/reflectivity, fluorescence and electron microscopy.

## NONBUNDLE-TO-BUNDLE TRANSITION OF TUBULIN TUBULES TRIGGERED BY TAU

Microtubules (MTs) are 25 nm protein nanotubes comprised of αβ tubulin subunits aligned end-to-end to form linear protofilaments which interact laterally to form hollow cylinders (1). Microtubules are highly anionic with the charge density of about 0.5 – 0.8 e/nm$^2$, and rigid with the persistence length of ~mm. Microtubules are involved in a variety of cellular functions of cell division, intracellular trafficking and maintaining cell shape. In eukaryotic cell division, microtubules exhibit dynamic instability, i.e., cycles of rapid shortening followed by slow growth. There are two distinct conformational transitions of tubulin, straight-to-curved transition in catastrophe. In catastrophe stage, GTPs are hydrolyzed into GDPs, then protofilaments are axially curved out and MTs are disassembled (2-4).

Neuronal MTs are highways for motor protein transporting cellular components from the body of the cell down to the end of the axon. MTs are long lived with microtubule-associated-protein (MAP) tau. MAP tau modulates microtubule dynamics by suppressing the rate of catastrophe. In Alzheimer's disease, tau is over-phosphorylated, then tau is detached from MTs, consequently MTs disintegrate, collapsing neuron's transport system (5). This results in malfunctions in communication between neurons and later, the death of the cells.

A chemotherapeutic drug paclitaxel (taxol) prevents disassembly of MTs by maintaining the straight conformation of GDP-tubulins (6). The previous study by atomic force microscopy (AFM) has revealed different curvatures of protoflilaments composed of GDP-tubulins with/without Taxol (7).

Microtubule bundles with string-like architectures were revealed in an axon initial segment (AIS) by electron microscopy (Fig. 1a) (8, 9). These 'fascicles of microtubules' are now considered to be the passage for kinesin motor proteins, which deliver neurotransmitters (10). While tau proteins are believed to interact with microtubules, how tau mediates the interaction between microtubules still needs to be elucidated. Widely spaced hexagonally ordered microtubules bundles were observed in non-neuronal cells with transfected tau cDNA but the studies could not conclude whether the bundles came from tau-mediated attraction or repulsive force under confinement (11, 12). In the case of in vitro studies with paclitaxel-stabilized microtubules, no microtubule bundles were observed (13-15).

In a work by Chung et al. (16), tau-mediated microtubule bundles with paclitaxel-free and active (i.e. hydrolyzing GTP) microtubules were studied using small angle X-ray scattering (SAXS) and transmission electron microscopy (TEM). In the SAXS study, widely spaced hexagonally ordered microtubule arrays with a wall-to-wall distance

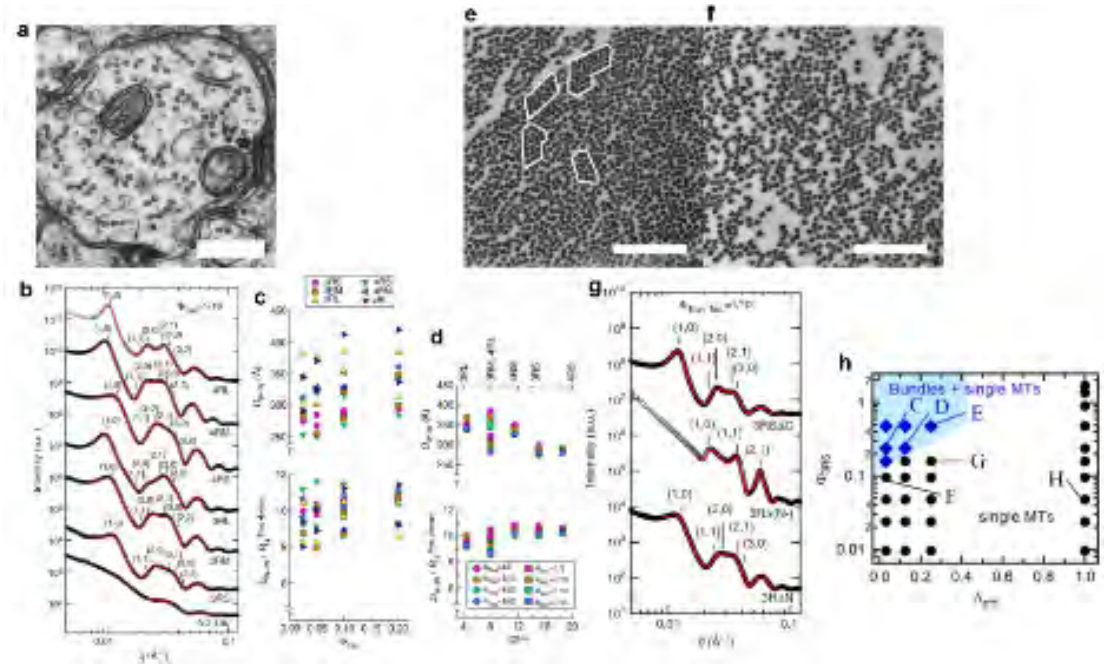


**Fig. 1:** Nonbunble-to-bundle transition of a microtubule triggered by tau proteins. (a) An electron microscopy image of a microtubule in the axon initial segment (AIS). Scale bar = 250 nm. (b) SAXS data of tau and microtubules for all six isoforms. (c) The wall-to-wall distance $d_{wall\text{-}to\text{-}wall}$ and $d_{wall\text{-}to\text{-}wall}$ normalized by the calculated radius of gyration of tau projection domain $R_G^{PD}$ for various ratios of six tau isoforms to tubulin. (d) The average $d_{wall\text{-}to\text{-}wall}$ and $d_{wall\text{-}to\text{-}wall}$ / $R_G^{PD}$ as a function of overall cationic charge of tau ($Q^{tau}$). (e,f) Cross sectional images of microtubule bundles with hexagonal ordering (e) and linear architecture (f). Scale bars = 500 nm. (g) SAXS data of truncated tau showing a collapsed microtubule bundle (middle) when an anionic block of tau is eliminated. (h) A phase diagram of microtubules as a function of Λ and Φ obtained from SAXS data with bundle phases at the shaded blue area.

$d_{wall\text{-}to\text{-}wall}$ = 25-41 nm were observed for 6 tau isoforms (Fig. 1b), which is consistent with the previously reported architecture in tau cDNA transfected cells. The ratio $d_{wall\text{-}to\text{-}wall}/R_{PD}$ was almost constant but the $d_{wall\text{-}to\text{-}wall}$ decreased as the overall cationic charge of tau increased (Fig. 1c,d). These findings indicate that the widely spaced bundles are affected by both tau PD size and the electrostatic interaction of tau. In plastic imbedded TEM images, cross sections of microtubule bundles with hexagonal ordering and string-like morphology were observed (Fig. 1e,f), where the latter corresponds with the architecture in AISs. The experiments using truncated tau showed that PD-truncated tau induced collapsed microtubule bundles with $d_{wall\text{-}to\text{-}wall}$ = 4-5 nm (Fig. 1g). This result indicates that the anionic block of PD plays a role as a repulsive barrier preventing microtubules from getting closer. Incidentally, tau whose entire NTT is truncated induces a widely spaced bundle with $d_{wall\text{-}to\text{-}wall}$ = 22-24 nm, which indicates that NTT is unnecessary for widely spaced bundles.

In the paper by Choi et al (17), the authors confirmed that paclitaxel, which has been widely used to stabilize microtubules for in vitro studies, acts as the opposite molecular switch for tau proteins. Using SAXS and TEM, they showed that the microtubules lost their hexagonal ordering as the ratio of paclitaxel to tubulin increased in the range of $1/32 \leq \Lambda \leq 1$ (Fig. 1h). At a low paclitaxel ratio < 1/4, microtubule doublets and triplets were observed as the concentration of tau increased, while microtubule bundles were absent when the ratio = 1. This study showed that the formation of microtubule bundles is highly affected by paclitaxel, so the elimination or minimization of paclitaxel is needed in order to study microtubule bundles that are related to in vivo properties.

The above studies reported two molecular switches regulating microtubule nonbundle-to-bundle transitions: MAP tau and paclitaxel. Quantitative analysis using SAXS provided insight into the energy landscape between the microtubules covered by tau proteins. In particular, they showed that the tau-mediated microtubule bundles are significantly related to the electrostatic interaction of tau projection parts. These studies provided a quantitative method to study the effect of tau dysfunction on microtubule bundle arrays by point mutation or hyperphosphorylation of tau.

## UNZIP-TO-ZIP TRANSITION OF LIPID MEMBRANES INDUCED BY SPAN 80

A cell membrane consists of complicated interactions between a variety of components, including proteins, lipids, and lipopolysaccharides. Although each of the components have important roles in the functionality of the cell membrane, it is a difficult task to investigate the role of individual components due to the overwhelming complexity of the interactions among the components. To solve this problem and to investigate desired components separately, techniques regarding the fabrication of a model system of the cell membrane have been developed for decades. (18-22) Despite all of the intensive research, however, there are still critical obstacles for model cell membrane fabrication. Among those obstacles, one of the most highlighted problems is the lack of stability of the freestanding lipid bilayer.

A bilayer is composed of self-assembled lipid molecules. A lipid is an amphiphilic molecule that has a hydrophilic head group and a hydrophobic tail group. When we prepare an oil-water interface using a lipid-dissolved, oily solvent and an aqueous solution, the lipid molecules are adsorbed to the interface to form a lipid monolayer due to its amphiphilic characteristics. Recent research developed a new method called the 'droplet interface bilayer' to fabricate a freestanding bilayer using this monolayer structure. (23-25) In this method, two monolayers are formed at the surface of two different water droplets in the lipid dissolved solvent. After monolayer formation, the droplets are moved toward each other until they touch and then the monolayers undergo a "zipping" process during which the two monolayers adhere to each other. During this monolayer to bilayer transition, however, it is frequent that a transient pore between the two monolayers is formed. Once this pore is formed between the monolayers, it expands due to the surface tension of the bilayer, resulting in the complete merging of the droplets. Therefore, it is necessary to prevent transient pore formation to fabricate stable freestanding lipid bilayers for general use.

A recent technique developed by Jeong et al. solved this problem by applying an oil-in-water emulsion stabilizer during the monolayer to bilayer transition. (26) In this technique, they formed a planar oil-water interface and water droplet using a solvent containing lipid and SPAN 80 (an oil-in-water emulsion stabilizer). Similar to the droplet interface bilayer, monolayers are formed on the planar oil-water interface and surface of the droplet. After the droplet touches the planar monolayer, a monolayer to bilayer transition occurs. Here, SPAN 80 plays an important role to prevent formation of a transient pore which has highly positive curvature because SPAN 80 has highly negative spontaneous curvature. As a result, an appropriate amount of SPAN 80 can insure stable transition from a monolayer to a bilayer. Interestingly, after the formation of the freestanding lipid bilayer, SPAN 80 moves out of the bilayer instead of remaining in. This phenomenon can be explained by adhesion between the two monolayers. Since the lipid monolayers have higher surface tension then half of the surface tension of the bilayer, the monolayer to bilayer transition is energetically favored. This energetic gain is the source of the adhesion between the two monolayers for the monolayer to bilayer transition. On the other hand, SPAN 80 does not have this adhesion to form the bilayer structure. Therefore, SPAN 80 spontaneously moves out from the bilayer since SPAN 80 prefers the monolayer state to the bilayer state.

As shown previously, a monolayer to bilayer transition can be affected by surfactants and their interactions. Spontaneous curvature, adhesion energy or other physical characteristics might determine how stably the transition occurs and how the components rearrange after the transition. This is why investigation of this transition process is important for many kinds of membrane-based research in the life sciences, physical sciences, and in biomedical engineering fields.

## RIPPLE-TO-LIQUID ORDERED ($L_O$) TRANSITION OF LIPID MEMBRANES REGULATED BY CHOLESTEROL

Cholesterol is a small amphiphilic molecule that consists a backbone structure of a cellular membrane with phospholipids. It has previously reported that cholesterol controls membrane structure and fluidity (27–30), thus being deeply involved in various cell functions such as signaling and disease development (31–34). Therefore, there have been numerous model studies for the phospholipid – cholesterol membrane by utilizing a wide range of optical, spectroscopy and diffraction techniques. In particular, the phase behavior of a dipalmitoylphosphatidylcholine (DPPC) – cholesterol membrane has been intensively studied due to its implication in lipid raft structure (35, 36).

By using synchrotron X-ray reflectivity, Lee et al. presents the enhancement of vertical order in DPPC multilayers by

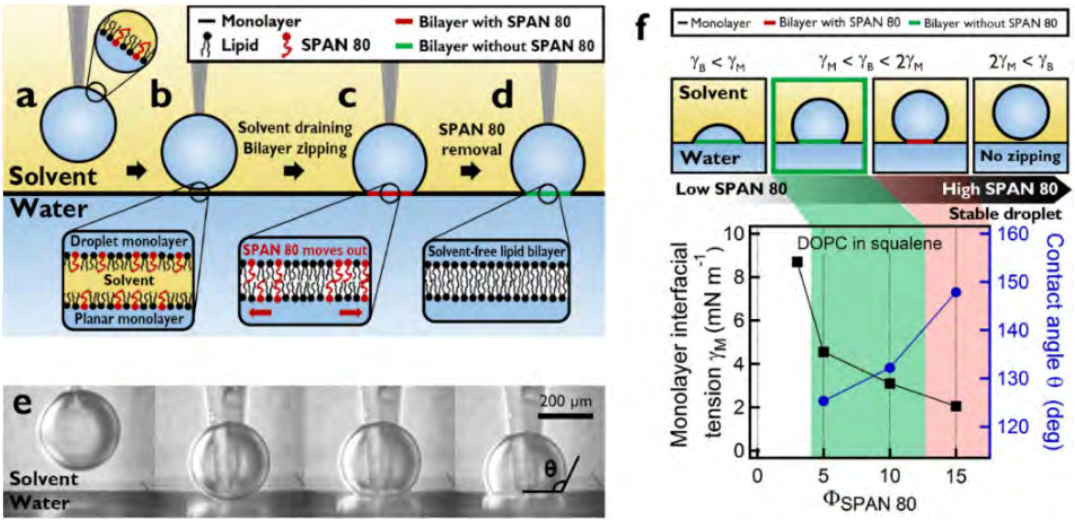


**Fig. 2:** (a-d) Schematics illustrating the formation of freestanding bilayer and spontaneous removal of the SPAN 80. (e) Side-view microscopy images in correspondence with each of (a-d). (f) Stability criteria for freestanding bilayer formation. Monolayer interfacial tension and contact angle for DOPC as a function of SPAN 80-to-lipid weight ratio $\Phi_{SPAN80}$. The regime of stable and SPAN 80-free bilayer is shown in green.

a cholesterol induced ripple-to-liquid ordered (Lo) phase transition. Until now, the majority of X-ray reflectivity studies on lipid – cholesterol systems were carried out with a monolayer configuration, which is far from the physiological condition, because it is hard to get a sufficient X-ray diffraction signal from the bilayers in an aqueous environment due to the X-ray absorption by the water. The authors utilized a lipid spin-coating method (37, 38) with a custom built X-ray liquid cell to solve this limitation. The DPPC – cholesterol mixture solution is first spin-coated on silicon wafer substrate, followed by the addition of a buffer solution and high temperature incubation. This process leads to the spontaneous formation of ~30 multibilayers on the wafer, which can amplify the X-ray diffraction signal from single bilayer to the multiple.

Fig. 3(a) shows raw X-ray reflectivity data from DPPC multilayers with various concentrations of cholesterol. The three major changes in reflectivity curves by adding more cholesterol are clearly shown – (i) q position shift, (ii) increased sharpness and (iii) increased amplitude of Bragg's peaks. We analyzed these features more specifically by converting them into the quantitative parameters. First, the lamellar spacing, which is the center-to-center distance between the bilayers, of DPPC – cholesterol lipid multilayers, are obtained from the q position of each Bragg's peak (Fig. 3(b)). As cholesterol concentration increases from 0 to 10%, the lamellar spacing rapidly increases about 10 Å, while further cholesterol addition to 50% slightly decreases the lamellar spacing. This 10 Å increase in lamellar spacing can be explained by the DPPC chain tilt-to-untilt transition due to the cholesterol insertion into the space between the chains. Secondly, the full width at half maximum (FWHM) of Bragg's peak as a function of cholesterol concentration is plotted in Fig. 3(c). FWHM has inverse proportional relationship with the sharpness of the peak, thus the rapid 4-fold decrease in FWHM from 3% to 10% of cholesterol concentration indicates the increase in peak sharpness at the same regime. Considering that FWHM is correlated with the vertical order of the sample, this decrease in FWHM indicates the certain transition of DPPC – cholesterol multilayers from a vertically disordered to well-ordered state. The electron density profiles for the 1, 5, 10, 30, and 50% of cholesterol concentration are shown in Fig. 3(d). The amplitude of the electron density profile increases about 8 times from 1 % to 50 % cholesterol, also implying the significant enhancement of vertical order in DPPC multilayers by adding cholesterol.

By summing up the detailed analysis on the X-ray reflectivity data for DPPC – cholesterol multilayers, we can conclude that DPPC multilayers, which are in a vertically disordered ripple phase, undergo the phase transition into vertically well-ordered $L_O$ phase by the addition of cholesterol. Fig. 3 shows schematics illustrating of this cholesterol induced phase transition. Note that DPPC multilayers with low cholesterol concentrations (< 10 %) are in a ripple phase, not in a simple gel phase. Although

the gel phase has a tilted chain, it cannot form a vertically disordered structure, it is reasonable to expect that the sample is in ripple phase with vertical undulation. We argue that this phase transition with vertical order enhancement is induced by the cholesterol, changing the conformation of the DPPC chains. Because the chain tilt-to-untilt transition (confirmed by lamellar spacing data) produces well aligned conformation of DPPC molecules, the structural undulation at the ripple phase disappears in the $L_o$ phase and the vertical order is improved (confirmed by FWHM and electron density data).

This finding suggests that the phase transition in lipid multilayers can cause structural change, not only in a lateral direction but also in a vertical direction, which is novel feature for investigating a model membrane. This research overcomes the previous limitations on studying the vertical order of membrane structure by using spin-coated lipid multilayers and an X-ray reflectivity experiment with customized X-ray liquid cell. It is expected that our study might inspire the importance of vertical structures in cell membrane and associated biological processes.

## OLIGOMER-TO-FIBRIL TRANSITION OF AMYLIN INHIBITED BY LIPOIC/ASCORBIC ACID

Protein misfolding and aggregation is of great significance as they are the hallmarks of various diseases, namely amyloidosis. (39, 40) The most well-known amyloid-related diseases include Alzheimer's disease, Parkinson's disease, and type 2 diabetes mellitus (T2DM). (41-43) In the case of T2DM, an amyloid deposit is observed in over 90 % of patients. (42, 44) Proteins exhibit abnormally increased beta-sheet conformation, which results in toxic fibrillation and extra/intracellular amyloid deposits. (43-45) Small (37 amino acids) proteins called amylins, which are secreted by pancreatic islet beta cells, are a major constituent of protein aggregation. (46) In normal conditions, amylin participates in the glycemic control system, co-secreted and acting synergistically with insulin. (47) However, in pathological situation, amylin aggregates to oligomeric and fibrillar forms and induces beta cell apoptosis. (43, 45, 48)

Although general pathways, including the "abnormal oligomer" seeding and fibril formation is known (Fig. 4(a)), the exact mechanism of amylin fibrillation has not been clearly discovered and, indeed, no inhibitors have been clinically approved. (45, 49) Various studies have

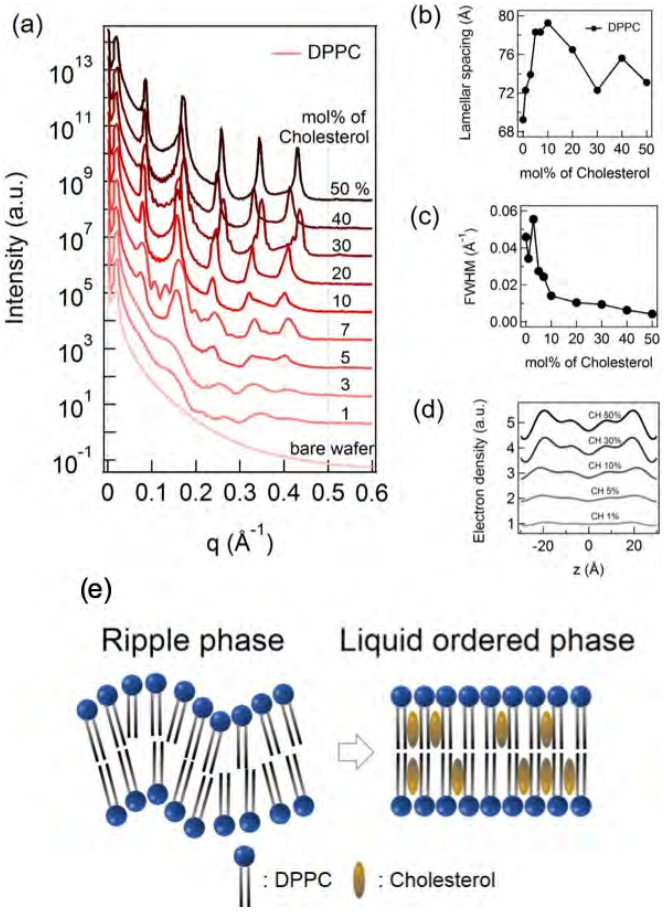


**Fig. 3:** (a) Synchrotron X-ray reflectivity data of DPPC-cholesterol multilayers. The position, intensity and sharpness of the X-ray structure factors of a DPPC multilayer are changed with increasing cholesterol concentration. (b) Lamellar spacing of DPPC-cholesterol multilayers vs. mol% of cholesterol. Lamellar spacing rapidly increases (≤ 10 % cholesterol) and then decreases (> 10 % cholesterol). (c) The full width at half maximum (FWHM) of a third order X-ray reflectivity peak of a DPPC-cholesterol multilayer. The FWHM decreases (i.e. X-ray peak sharpening) with increasing mol % of cholesterol. (d) Representative electron density of a DPPC-cholesterol multilayer at 1, 5, 10, 30, 50 % cholesterol. This imply that the vertical order of a DPPC multilayer at low cholesterol is enhanced by adding cholesterol. (e) Schematics illustrating vertical order enhancement caused by cholesterol-induced phase transition of a DPPC multilayer. The DPPC multilayer is in a ripple phase in a low cholesterol regime (0 – 10 %). With increasing cholesterol concentration, the ripple-to-$L_o$ phase transition occurs and the vertical order between layers is enhanced.

suggested that the pH conditions are related to the fibrillation process. (45, 50, 51) An acidic pH condition has been shown to reduce the aggregation rate of amylin, compared with physiological pH condition of 7.4. (50-52)

Recently, Azzam et al. have specifically screened total six acidic small molecules: acetylsalicylic acid, ascorbic acid, benzoic acid, folic acid, lipoic acid, salicylic acid and have discovered that ascorbic acid and lipoic acid have a signif-

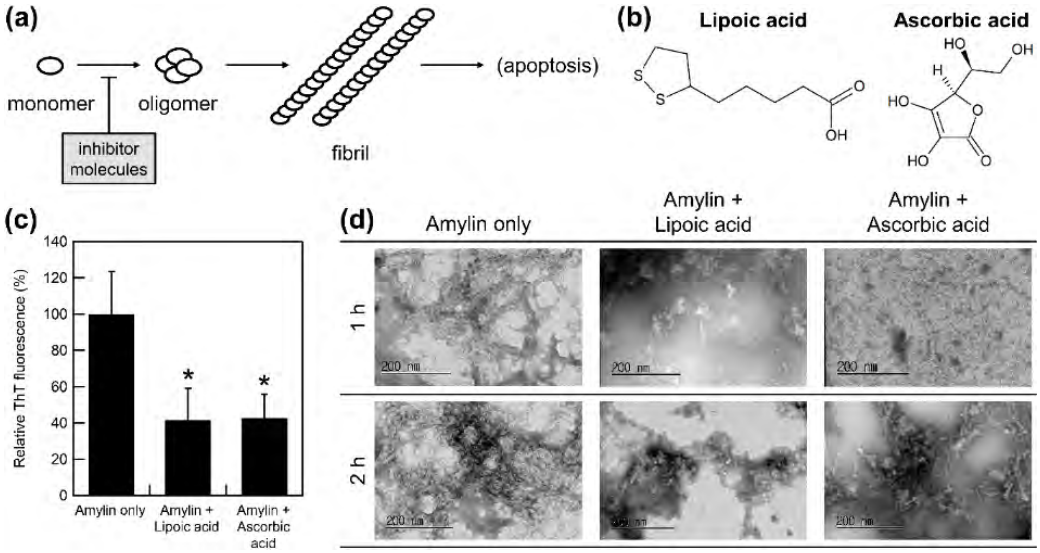


**Fig. 4:** Inhibition of amylin aggregation with acid compounds. (a) Schematics of the toxic effect of amylin aggregation and its inhibition. Inhibitor molecules can hinder the formation of oligomeric form, thus preventing subsequent pathological effects. (b) Molecular structures of suggested inhibitor molecules: lipoic acid and ascorbic acid. (c) Relative ThT fluorescence of amylin solution (15 μM) after 2 h incubation at 37 °C with and without acid molecules (15 μM). (d) TEM images of an amylin solution with and without acid molecules. Samples were negatively stained with uranyl formate after 1 h or 2 h incubation.

icant effect on inhibiting human amylin fibril formation (Fig. 4(b)). (45) In particular, beta sheet conformation i.e. the amount of amyloid fibril was quantified by measuring relative intensity of thioflavin T (ThT) fluorescence, whereas the nanoscopic protein fibril structures were then compared with transmission electron microscopy (TEM). The inhibitory effects of acidic molecules were significant. Both the addition of lipoic acid and ascorbic acid decreased the ThT fluorescence to 42.1 ± 17.2% and 42.9 ± 12.8% respectively, compared with control (Fig. 4(c)). Consistent with the ThT assay, TEM images also showed time-dependent reduction in both number and length of amylin fibrils in the presence of lipoic acid and ascorbic acid (Fig. 4(d)). The authors also further assessed the mechanism of inhibition by the cellular toxicity test and a molecular dynamics simulation. (45)

It is known that rodent amylin, which contains proline in Ser20-Ser29 region is non-amyloidogenic. (45, 47, 53) This is because proline prevents beta sheet formation by enhancing amino acid chain rigidity, as also confirmed in amyloid beta and other fibril-forming proteins. (47, 54) Azzam et al. demonstrated that both lipoic acid and ascorbic acid can bind to or interact with hydrophobic residues such as Ser28, Gly24, and Leu27, stabilizing the structure of amylin monomers. (45) It is expected that this finding will provide useful insights for the pharmaceutical field. It is also notable that TEM imaging, combined with other assays, can be practically utilized as a standardized screening method for molecular agents that alter the protein structures (fibrils or assembly structures), in either a beneficial or harmful way.

**Acknowledgments:** This work was supported by NRF-2017M2A2A6A01071190, NRF-2018R1A2B3001690, KC30 N11170021, KUSTAR-KAIST Institute, KAERI and APCTP.

### *References*

[1] T. Fojo, The Role of Microtubules in Cell Biology, Neurobiology, and Oncology (2008).
[2] J. Howard, A. a Hyman, Dynamics and mechanics of the microtubule plus end. Nature. 422, 753–8 (2003).
[3] E. Nogales, H.-W. Wang, Structural mechanisms underlying nucleotide-dependent self-assembly of tubulin and its relatives. Curr. Opin. Struct. Biol. 16 (2006), pp. 221–9.
[4] E. Nogales, H.-W. Wang, Structural intermediates in microtubule assembly and disassembly: how and why? Curr. Opin. Cell Biol. 18 (2006), pp. 179–84.
[5] Kosik, K. S., Joachim, C. L. & Selkoe, D. J. Microtubule-associated protein tau (tau) is a major antigenic component of paired helical filaments in Alzheimer disease. Proc. Natl Acad. Sci. USA 83, 4044–4048 (1986).
[6] Choi, M.C. et al. Human microtubule-associated-protein tau regulates the number of protofilaments in microtubules: A synchrotron X-ray scattering study. Biophys. J. 97, 519–527 (2009).
[7] Elie-Caille, C. et al. Straight GDP-tubulin protofilaments form in the presence of taxol. Curr. Biol. 17, 1765–1770 (2007).
[8] Peters, A., Palay, S. L. & Webster, H. deF. The Fine Structure of the Nervous System: Neurons and Their Supporting Cells (Oxford Univ. Press, 1991).

[9] Palay, S. L., Sotelo, C., Peters, A. & Orkand, P. M. The axon hillock and the initial segment. J. Cell Biol. 38, 193–201 (1968).
[10] Rasband, M. N. The axon initial segment and the maintenance of neuronal polarity. Nat. Rev. Neurosci. 11, 552–562 (2010).
[11] Chen, J., Kanai, Y., Cowan, N. J. & Hirokawa, N. Projection domains of MAP2 and tau determine spacings between microtubules in dendrites and axons. Nature 360, 674–677 (1992).
[12] Baas, P. W., Pienkowski, T. P. & Kosik, K. S. Processes induced by tau expression in Sf9 cells have an axon-like microtubule organization. J. Cell Biol. 115, 1333–1344 (1991).
[13] Gustke, N., Trinczek, B., Biernat, J., Mandelkow, E. M. & Mandelkow, E. Domains of tau protein and interactions with microtubules. Biochemistry 33, 9511–9522 (1994).
[14] Brandt, R. & Lee, G. Orientation, assembly, and stability of microtubule bundles induced by a fragment of tau protein. Cell Motil. Cytoskeleton 28, 143–154 (1994).
[15] Choi, M. C. et al. Human microtubule-associated-protein tau regulates the number of protofilaments in microtubules: a synchrotron X-ray scattering study. Biophys. J. 97, 519–527 (2009).
[16] Chung, P. J. et al. Tau Mediates Microtubule Bundle Architectures Mimicking Fascicles of Microtubules found in the Axon Initial Segment. Nautre Commun. 7, 1–9 (2016).
[17] Choi, M. C. et al. Paclitaxel suppresses Tau-mediated microtubule bundling in a concentration-dependent manner. Biochim. Biophys. Acta - Gen. Subj. 1861, 3456–3463 (2017).
[18] McConnell, H. M. & Kornberg, R. D. Inside-outside transitions of phospholipids in vesicle membranes. Biochemistry 10, 1111–1120 (1971)
[19] Pautot, S., Frisken, B. J. & Weitz, D. Engineering asymmetric vesicles. Proceedings of the National Academy of Sciences 100, 10718–10721 (2003).
[20] Sackmann, E. Supported membranes: scientific and practical applications. Science 271, 43 (1996).
[21] Mueller, P., Rudin, D. O., Ti Tien, H. & Wescott, W. C. Reconstitution of cell membrane structure in vitro and its transformation into an excitable system. Nature 194, 979–980 (1962).
[22] Mey, I. et al. Local membrane mechanics of pore-spanning bilayers. Journal of the American Chemical Society 131, 7031–7039 (2009).
[23] Thiam, A. R., Bremond, N. & Bibette, J. From stability to permeability of adhesive emulsion bilayers. Langmuir 28, 6291–6298 (2012).
[24] Leptihn, S. et al. Constructing droplet interface bilayers from the contact of aqueous droplets in oil. Nature protocols 8, 1048–1057 (2013).
[25] Boreyko, J. B., Polizos, G., Datskos, P. G., Sarles, S. A. & Collier, C. P. Air-stable droplet interface bilayers on oil-infused surfaces. Proceedings of the National Academy of Sciences 111, 7588–7593 (2014).
[26] Jeong, D.-W., Jang, H., Choi, S.Q. & Choi, M.C. Enhanced stability of freestanding lipid bilayer and its stability criteria. Scientific Reports 6, 38158 (2016)
[27] P. L. Yeagle, Cholesterol and the cell membrane. BBA - Rev. Biomembr. 822, 267–287 (1985).
[28] P. L. Yeagle, Modulation of membrane function by cholesterol. Biochimie. 73, 1303–1310 (1991).
[29] A. Chabanel, M. Flamm, K. L. P. Sung, Influence of cholesterol content on red cell membrane viscoelasticity and fluidity. Biophys. J. 44, 171–176 (1983).
[30] R. A. Cooper, E. C. Arner, J. S. Wiley, S. J. Shattil, Modification of red cell membrane structure by cholesterol-rich lipid dispersions. A model for the primary spur cell defect. J. Clin. Invest. 55, 115–126 (1975).
[31] S. Parpal, M. Karlsson, H. Thorn, P. Strålfors, Cholesterol depletion disrupts caveolae and insulin receptor signaling for metabolic control via insulin receptor substrate-1, but not for mitogen-activated protein kinase control. J. Biol. Chem. 276, 9670–8 (2001).
[32] D. Papahadjopoulos, Role of cholesterol in membranes effects on phospholipid-protein interactions, membrane permeability and enzymatic activity. Biochim. Biophys. Acta. 330, 8–26 (1973).
[33] K. Simons, R. Ehehalt, Cholesterol, lipid rafts, and disease. J. Clin. Invest. 110, 597–603 (2002).
[34] J. Silvius, Role of cholesterol in lipid raft formation: lessons from lipid model systems. Biochim. Biophys. Acta - Biomembr. 1610, 174–183 (2003).
[35] G. van Meer, D. R. Voelker, G. W. Feigenson, Membrane lipids: where they are and how they behave. Nat. Rev. Mol. Cell Biol. 9, 112–24 (2008).
[36] K. Simons, E. Ikonen, Functional rafts in cell membranes. Nature. 387, 569–72 (1997).
[37] U. Mennicke, T. Salditt, Preparation of Solid-Supported Lipid Bilayers by Spin-Coating. Langmuir. 18, 8172–8177 (2002).
[38] A. C. Simonsen, L. a Bagatolli, Structure of spin-coated lipid films and domain formation in supported membranes formed by hydration. Langmuir. 20, 9720–8 (2004).
[39] J. D. Sipe et al., Nomenclature 2014: Amyloid fibril proteins and clinical classification of the amyloidosis. Amyloid 21, 221-224 (2014).
[40] Y. S. Eisele et al., Targeting protein aggregation for the treatment of degenerative diseases. Nat Rev Drug Discov 14, 759-780 (2015).
[41] M. P. Mattson, Pathways towards and away from Alzheimer's disease. Nature 430, 631-639 (2004).
[42] F. Chiti, C. M. Dobson, Protein misfolding, functional amyloid, and human disease. Annu Rev Biochem 75, 333-366 (2006).
[43] L. Haataja, T. Gurlo, C. J. Huang, P. C. Butler, Islet amyloid in type 2 diabetes, and the toxic oligomer hypothesis. Endocr Rev 29, 303-316 (2008).
[44] T. Sanke, G. I. Bell, C. Sample, A. H. Rubenstein, D. F. Steiner, An Islet Amyloid Peptide Is Derived from an 89-Amino Acid Precursor by Proteolytic Processing. J Biol Chem 263, 17243-17246 (1988).
[45] S. K. Azzam et al., Inhibition of Human Amylin Aggregation and Cellular Toxicity by Lipoic Acid and Ascorbic Acid. Mol Pharm 15, 2098-2106 (2018).
[46] A. N. Roberts et al., Molecular and functional characterization of amylin, a peptide associated with type 2 diabetes mellitus. Proc Natl Acad Sci U S A 86, 9662-9666 (1989).
[47] L. Caillon, A. R. Hoffmann, A. Botz, L. Khemtemourian, Molecular Structure, Membrane Interactions, and Toxicity of the Islet Amyloid Polypeptide in Type 2 Diabetes Mellitus. J Diabetes Res 2016, 5639875 (2016).
[48] C. A. Jurgens et al., beta-cell loss and beta-cell apoptosis in human type 2 diabetes are related to islet amyloid deposition. Am J Pathol 178, 2632-2640 (2011).
[49] A. Abedini, A. M. Schmidt, Mechanisms of islet amyloidosis toxicity in type 2 diabetes. FEBS Lett 587, 1119-1127 (2013).
[50] H. R. Jeong, S. S. An, Causative factors for formation of toxic islet amyloid polypeptide oligomer in type 2 diabetes mellitus. Clin Interv Aging 10, 1873-1879 (2015).
[51] L. Khemtemourian, E. Domenech, J. P. F. Doux, M. C. Koorengevel, J. A. Killian, Low pH Acts as Inhibitor of Membrane Damage Induced by Human Islet Amyloid Polypeptide. J Am Chem Soc 133, 15598-15604 (2011).
[52] A. T. Alexandrescu, S. Jha, J. M. Snell, S. R. Sheftic, The pH-Dependence of Amylin Fibrillization. Biophys J 104, 360a-360a (2013).
[53] R. L. Hull, G. T. Westermark, P. Westermark, S. E. Kahn, Islet amyloid: a critical entity in the pathogenesis of type 2 diabetes. J Clin Endocrinol Metab 89, 3629-3643 (2004).
[54] S. J. Wood, R. Wetzel, J. D. Martin, M. R. Hurle, Prolines and amyloidogenicity in fragments of the Alzheimer's peptide beta/A4. Biochemistry-Us 34, 724-730 (1995).

**Daewoong Jeong** is a research associate at the Department of Bio and Brain Engineering at KAIST. He received PhD in Bio and Brain Engineering with research on fabrication and analysis of model cell membrane from KAIST. After receiving the PhD, he worked at NOTA Co. as CEO before joining the Department of Bio and Brain Engineering in KAIST. His current research field is engineering of self-assembled nano material.

**Suho Lee** is a postdoctoral researcher in the Department of Bio and Brain Engineering at KAIST. He received his BS, MS and PhD in Bio and Brain Engineering at KAIST in 2012, 2014 and 2019, respectively. His research mainly focuses on the structural transition of lipid membranes associated with the lipid raft hypothesis.

**Juncheol Lee** is a PhD candidate in the Department of Bio and Brain Engineering at KAIST. His research field is protein-based nanomaterials science and engineering.

**Hyunwoo Jang** is a research associate in the Department of Bio and Brain Engineering at KAIST. He completed his BS and MSc in Bio and Brain Engineering from KAIST in 2015 and 2018, respectively. After receiving his MSc, he became a research associate in the same laboratory. His main area of research interest is the self-association and aggregation of amyloidogenic proteins, especially those related with Alzheimer's disease.

**Sungmun Lee** is an associate professor of biomedical engineering at the Healthcare Engineering Innovation Center (HEIC) at Khalifa University. He completed his BS in chemical engineering from Korea University in 1996 and received a MSc in chemical engineering from Seoul National University in 1999. He went on to complete his PhD at Texas A&M University in 2005. He conducted post-doctoral work at the Georgia Institute of Technology until 2011 before becoming an assistant professor at Khalifa University. At Khalifa University, his research has focused on the development of novel drugs and drug delivery systems for treating Alzheimer's disease, diabetes, and cardiovascular diseases.

**Myung Chul Choi** is an associate professor of the Department of Bio and Brain Engineering at KAIST. He received PhD in physics in 2000 from KAIST for his work on "Confinement Effects on Mesoscopic Structures of Macromolecules". He joined the faculty of KAIST in 2010. His group's research is focused on elucidating assembly structures and interactions of biological molecules (eg. lipid membranes, microtubules, etc.) by using X-ray scattering, electron microscopy, and optical trapping experiments.